



Predicting Organic–Inorganic Aerosol Efflorescence Using Thermodynamically Modeled Viscosity

Shanshan Chen¹, Qishen Huang^{1*}, Ying Li^{2,3}, Shu-Feng Pang¹, Pai Liu¹, Yun-Hong Zhang¹

5 ¹ State Key Laboratory of Environment Characteristics and Effects for Near-space, School of Chemistry and Chemical Engineering, Beijing Institute of Technology, Beijing, 100081, China

² School of Environmental Science and Technology, Dalian University of Technology, Dalian, 1116024, China

10 ³ Key Laboratory of Atmospheric Environment and Extreme Meteorology, Institute of Atmospheric Physics, Chinese Academy of Sciences, Beijing 100029, China

Correspondence: Qishen Huang (qishenh@bit.edu.cn)

Abstract. Atmospheric aerosols, especially internally mixed organic–inorganic aerosols, exhibit complex phase behaviors that affect their size evolution, optical properties, and chemical reactivity, ultimately impacting climate and human health. Although parameterizations for secondary organic aerosol phase 15 state exist, predictive models based on primary predictors for efflorescence in organic–inorganic aerosols remain underdeveloped. In this study, we evaluated several chemical parameters, including equivalent O:C ratio, organic mass fractions, glass transition temperature (T_g), and viscosity (η), and identified aerosol viscosity as the primary predictor of efflorescence relative humidity (ERH) in internally mixed organic–inorganic aerosols. We developed a linear viscosity–ERH model based on ERH and $\log_{10} \eta$, 20 which defines the boundary conditions for aerosol efflorescence when $\eta < 4.76 \times 10^2 \text{ Pa}\cdot\text{s}$. Additionally, we showed that efflorescence is inhibited when $\eta > 4.76 \times 10^2 \text{ Pa}\cdot\text{s}$. Validation using an independent dataset showed strong agreement between predicted and experimentally measured ERH ($R^2 = 0.95$). A multivariate regression model incorporating η and T_g improved prediction accuracy but was limited by T_g parameterization for complex organic–inorganic mixtures. Our findings highlight the role of aerosol 25 viscosity in controlling efflorescence and emphasize the need to develop improved aerosol viscosity measurement techniques to better constrain aerosol phase transitions in atmospheric models.



1 Introduction

30 Atmospheric aerosols significantly influence climate and human health through both direct and indirect effects. They directly influence the energy balance by absorbing and scattering solar radiation and indirectly affect the climate by acting as cloud condensation nuclei (CCN), thereby altering cloud microphysical properties such as droplet size, lifetime, and optical characteristics. (Boreddy et al., 2014; Fan et al., 2010; Knopf and Alpert, 2023; Novo et al., 2021; Pöschl, 2005; Shrivastava et al., 2017; Smith et al., 2021) Among aerosol physicochemical properties, phase state (liquid, solid, or semi-solid) is particularly important, as it governs hygroscopicity, optical properties, and heterogeneous reactivity. (Fard et al., 2018; Freedman et al., 2024; Novo et al., 2021) Moreover, aerosol phase transition significantly affects viral activity during transmission(Oswin et al., 2022). Consequently, aerosol phase states substantially impact climate, air quality, and human health(Reid et al., 2018).

40 Atmospheric aerosols, particularly internally mixed secondary aerosols composed of organic and inorganic components, exhibit diverse phase states, including liquid, liquid-liquid phase-separated, semi-solid, amorphous solid, and crystalline solid, which governs their physicochemical properties.(Novo et al., 2021) For instance, aerosols undergoing efflorescence (i.e., crystallization) and deliquescence exhibit hysteresis in particle size and water content in response to relative humidity (RH) variations.(Choi and Chan, 2002; Guo et al., 2020) In contrast, amorphous organic aerosols show no hysteresis behavior in their hygroscopic growth. Thus, effloresced (or crystallized) aerosols display fundamentally different hygroscopic behaviors from amorphous ones, introducing substantial uncertainties in aerosol hygroscopicity under varying RH conditions.

45 However, internally-mixed organic-inorganic aerosols are chemically complex, often containing thousands of distinct organic species, of which only about 10% have been identified.(Hallquist et al., 2009) This limited chemical characterization constrains our ability to accurately predict aerosol phase states. Existing parameterization models based on organic aerosol properties, such as molecular weight and oxygen-to-carbon ratio (O:C ratio)(Shiraiwa et al., 2017), elemental composition(DeRieux et al., 2018), and volatility(Li et al., 2020a; Zhang et al., 2019) to predict the glass transition temperature (T_g)

50 have been established to predict the viscosity and phase state of organic aerosols but these models typically neglect efflorescence. Consequently, current parameterizations fail to distinguish between crystalline and amorphous solid states of internally mixed organic-inorganic aerosols and overlook the



hysteresis in particle size and water uptake during efflorescence-deliquescence cycles. This limitation introduces significant uncertainty in predicting aerosol size evolution and lead to biases in describing atmospheric aerosol phase behavior, hygroscopicity, and optical properties, ultimately affecting our understanding of atmospheric particle aging, CCN activation, as well as climate and health impacts.

While laboratory studies have provided substantial data on efflorescence in mixed organic-inorganic aerosols, a systematic understanding of the key factors that govern and predict efflorescence remains limited. Efflorescence is a kinetically-controlled process that requires overcoming a nucleation energy barrier, which depends on factors such as component diffusion (e.g., viscosity), chemical composition (e.g., concentration, solubility, and vapor pressure), molecular interactions, and interfacial interactions such as surface tension.(Davis et al., 2015; Ma et al., 2021a; Mikhailov et al., 2009) The transition point, described by the efflorescence relative humidity (ERH), is therefore strongly influenced by these factors, which are modulated by the properties of organic components, and the hydration state of the inorganic salts. The O:C ratio is widely used as a parameter for organic compound polarity.(Yu et al., 2021) Previous studies have shown that increasing the mass fraction of organic compounds (ω_{org}), particularly with high-viscosity organics, can significantly alter mass transport processes, and thereby affect phase transition.(Parsons et al., 2004; Shiraiwa et al., 2013; Virtanen et al., 2010; Wang et al., 2017a; Zobrist et al., 2011) Under such conditions, aerosols may shift from efflorescence behavior to amorphous phase transitions similar to glass transitions at the glass transition temperature (T_g).(Berkemeier et al., 2016; Koop et al., 2011a; Song et al., 2016b; Tong et al., 2011) However, direct and reliable measurement for atmospheric aerosols remain challenging(Fitzgerald et al., 2016; Hosny et al., 2016a), resulting in limited observational data and motivating the use of thermodynamic models, such as AIOMFAC, to predict the viscosity of organic-inorganic mixture aerosols.(Lilek and Zuend, 2022a)

In this study, we develop a parameterization for predicting the ERH of organic-inorganic aerosols by integrating literature-reported ERH data, by investigating different aerosol physicochemical parameters, focusing on aerosol viscosity (η) and the collective effect of O:C ratio, ω_{org} , and T_g . The established framework enhances our understanding of aerosol phase behavior and size change during hygroscopic cycles, offering valuable insights into atmospheric processes, such as gas-particle partitioning, heterogeneous chemistry, and cloud formation.



2 Methods

2.1 The dataset for the parameterization

We compiled aerosol ERH data from our previous studies and peer-reviewed literature identified through Web of Science using keywords: aerosol, hygroscopic, and efflorescence. All studies were laboratory based, with ERH measured using IR spectroscopy(Braban and Abbatt, 2004; Cai et al., 2017; Ghorai et al., 2014; Ji et al., 2017a; Ma et al., 2021b; Ren et al., 2016; Shi et al., 2017; Wang et al., 2017a; Wu, 2017; Xu et al., 2022), Raman spectroscopy(Chang, 2020; Hu et al., 2025; Ushijima et al., 2021; Wang, 2018; Yu et al., 2012), optical microscope(Bertram et al., 2011; Huang et al., 2024; Parsons et al., 2004) or Hygroscopicity Tandem Differential Mobility Analyzer (HTDMA)(Laskina et al., 2015)

90 A total of 102 ERH data points for organic-inorganic mixture aerosols were collected: 66 ERH points for the training set (Table S1) and the remaining 36 points for the validation set (Table S2). The training set includes aerosol compositions containing 14 organic compounds (composed of C, H, and O) and 4 inorganic salts (ammonium sulfate, ammonium nitrate, sodium chloride, and potassium chloride) mixed in varying ratios. The validation set contains 36 ERH data from systems involving 12 organic compounds

100 and 4 inorganic salts (Table S2), selected from studies that either reported both aerosol ERH and viscosity reported or observed no efflorescence.

Key physicochemical parameters for predicting aerosol ERH include the equivalent O:C ratio of the mixture ($O:C_{mixture} = \left(\frac{n_{O,org}}{n_{C,org}} \right) \cdot x_{org}$, where x_{org} is the organic molar fraction ($x_{org} = \frac{n_{org}}{n_{org} + n_{inorg}}$), and $n_{inorg} = 0$ mol for purely organic aerosols (making $O:C_{mixture} = O:C$)). Other parameters include ω_{org} , 105 fractional T_g at ERH ($T_{g(\omega_{org})}$), and viscosity.

2.2 AIOMFAC model

Aerosol viscosity at the corresponding ERH and 298 K was estimated using the Aerosol Inorganic-Organic Mixtures Functional groups Activity Coefficients (AIOMFAC) model.(Zuend et al., 2008, 2011a). AIOMFAC is a thermodynamics-based group-contribution framework developed for aqueous 110 organic-inorganic mixtures. It predicts dynamic viscosity based on Eyring's absolute rate theory, which relates viscosity to the molar Gibbs energy of activation for viscous flow (Δg^*). Adopting the UNIFAC concept, AIOMFAC segments organic molecules into functional subgroups, treating the liquid mixture



as a 'solution of groups' to manage chemical complexity. The total (Δg^*) is derived from the additive contributions of these organic functional groups (based on the method by Gervasi et al.) and inorganic ions, accounting for temperature, ion activities, and ionic strength. For the organic-inorganic mixtures, the model applies the electrolyte-aware water pseudo-component ("aquelec") mixing approach, which effectively captures ion-solvent interactions.(Fredenslund et al., 1975; Hansen et al., 1991; Lilek and Zuend, 2022b; Zuend et al., 2011b). Validation against experimental viscosity data for sucrose–nitrate systems demonstrated that the aquelec approach accurately characterizes the viscosity of internally mixed organic–inorganic aerosols, establishing AIOMFAC-VISC as a robust tool for predicting atmospheric aerosol viscosity when experimental measurements are unavailable.(Lilek and Zuend, 2022b)

Accordingly, viscosity calculations were performed by specifying the functional groups of the organic components, inorganic salt composition, organic-to-inorganic ratio (OIR), and a series of organic molar fractions (X_{org}) ranging from 0.01 to 0.99 in increments of 0.01. For each system, the viscosity corresponding to the water activity closest to the literature reported ERH (within $\pm 0.5\%$ RH) was selected. For example, in a 1,2,6-hexanetriol and ammonium sulfate (1:1) mixture, we defined 1,2,6-hexanetriol as 2 CH₂, 1 CH OH, 3 CH₂ and 3 OH. The viscosity of the mixture system was achieved at aw = 0.47, which closely matches the ERH value in the literature (47.4%). Functional group definitions for all organic components are listed in Table S3. To assess the uncertainty associated with the thermodynamic state predictions, the sensitivity of viscosity ($\pm \log_{10}(\eta \text{ sens.}/[\text{Pa.s}])$) was calculated for each mixture. This metric quantifies the variation in predicted viscosity resulting from a $\pm 2\%$ perturbation in aerosol water mass fraction and serve as a proxy uncertainty related to compositional variability. The corresponding values are listed in Table S1.

2.3 Calculation of the fractional glass transition temperature ($T_{\text{g}}(\text{toorg})$)

Multiple parameterizations exist for estimating the glass transition temperature (T_{g}) of organic compounds, based on either volatility melting point (T_{m})(Galeazzo and Shiraiwa, 2022; Koop et al., 2011b; Li et al., 2020b). Herein, we elected the volatility-based parameterization developed by Li et al. (Eq.1), which predicts T_{g} from the saturation mass concentration (C^0), since T_{g} values predicted by Eq. 1 show closer agreement with literature data and smaller errors compared to T_{m} -based methods (Table S4) for representative organics.(Armeli et al., 2023; Li et al., 2020a) Moreover, the C^0 based method is broadly applicable, particularly when the O:C ratio is unavailable for complex organic mixtures.



$$T_g = 288.7 - 15.33 \times \log_{10}(C^0) - 0.33 \times [\log_{10}(C^0)]^2 \quad (1)$$

C^0 was estimated as a function of C, O, N, S numbers of the organic compound ($\log_{10}C^0 = f(n_C, n_O, n_N, n_S)$, Eq. 2): (Donahue et al., 2011; Li et al., 2016)

145
$$\log_{10} C^0 = (n_C^0 - n_C)b_C - n_O b_O - 2 \frac{n_C n_O}{n_C + n_O} b_{CO} - n_N b_N - n_S b_S. \quad (2)$$

Here, n_C^0 is the reference carbon number; n_C , n_O , n_N , and n_S denote the number of carbon, oxygen, nitrogen, and sulfur atoms, respectively; b coefficients (b_C , b_O , b_N , and b_S) denote atomic contributions fitted via multi-linear least squares analysis from 30,000 compounds across multiple classes(CH, CHO, CHN, CHON, CHOS, and CHONS)(Li et al., 2016). b_{CO} represents the carbon-oxygen nonideality.

150 Since inorganic salts involved in this study do not exhibit T_g due to crystallization, we applied the fractional T_g of organic-water mixtures ($T_g(\omega_{org})$) to account for the effect of mixing. $T_g(\omega_{org})$ was calculated using the Gordon-Taylor equation:(Gordon and Taylor, 1952)

$$T_g(\omega_{org}) = \frac{(1 - \omega_{org})T_{g,w} + \frac{1}{k_{GT}}\omega_{org}T_{g,org}}{(1 - \omega_{org}) + \frac{1}{k_{GT}}\omega_{org}} \quad (3)$$

155 where ω_{org} is the organic mas fraction calculated via the AIOMFAC model at aerosol ERH, $T_{g,w}$ is the glass transition temperature of pure water (136 K),(Kohl et al., 2005) and k_{GT} (the Gordon-Taylor constant) was assumed to be 2.5 for organic-water mixtures. (Koop et al., 2011a; Zobrist et al., 2008)

3 Results and Discussion

3.1 Correlation between ERH and physicochemical parameters

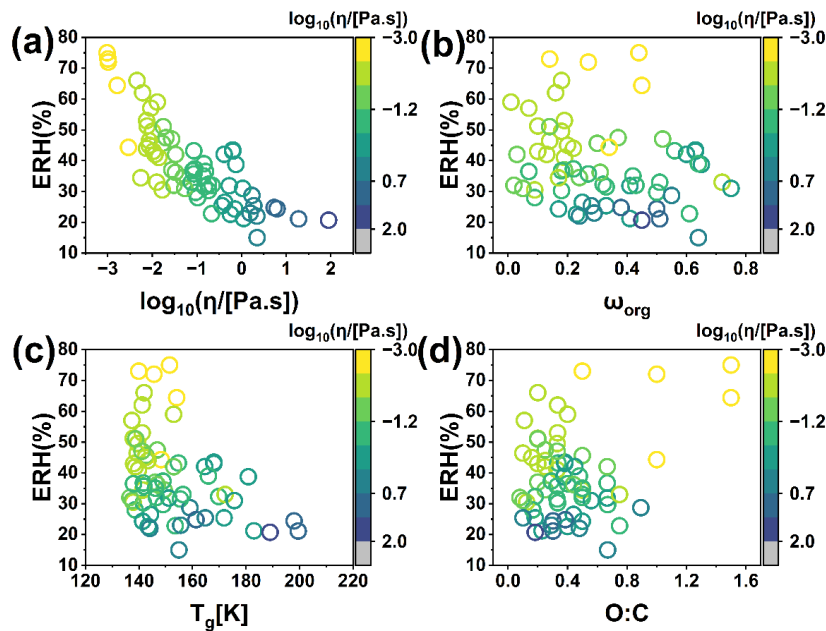
160 The efflorescence process of atmospheric aerosols is primarily controlled by the nucleation and crystal growth (i.e., crystallization) of inorganic salts within aerosol particles. Variations in aerosol ERH largely reflect the influence of organic components on inorganic salt crystallization. Therefore, we examined the correlation between ERH and key physicochemical parameters describing the organic components in organic-inorganic mixture aerosols: O:C ratio, ω_{org} , and $T_g(\omega_{org})$ (Figure.1).

165 Linear regression analysis using the training set (66 data points) showed no significant correlations between aerosol ERH and any of O:C, ω_{org} , or $T_g(\omega_{org})$ individually ($R^2 < 0.15$; Table S5). Multivariate regression considering the combined influence of three parameters provided only a limited improvement ($R^2 = 0.25$, Table S6).

When we color-coded the training dataset in Figure 1b-1d based on aerosol viscosity (the logarithm of



viscosity estimated using the AIOMFAC, $\log_{10} \eta$), a clear trend emerged: aerosols with lower viscosity
 170 generally exhibited higher ERH, while those with higher viscosity tended to have lower ERH. This trend
 is further supported by the scatter plot of aerosol ERH versus viscosity (Figure 1a), which shows an
 apparent negative correlation. These results indicate that viscosity may play a key regulatory role in
 aerosol efflorescence and could be a critical predictor for ERH.



175 **Figure 1.** Relationships between the ERH of organic-inorganic mixed aerosols. (a) the logarithm of viscosity ($\log_{10}(\eta/[Pa \cdot s])$), (b) the organic mass fraction (ω_{org}), (c) the glass transition temperature ($T_g(\omega_{org})$, K), and (d) O:C ratio. The color bar denotes the aerosol viscosity in $\log_{10}(\eta/[Pa \cdot s])$.

3.2 ERH prediction using viscosity

Building on the correlation between viscosity and ERH observed in Figure 1, we developed a linear
 180 regression model using the training set (Figure 2). The fitted equation is

$$ERH(\eta) = -10.23 \cdot \log_{10} \eta + 27.40 \quad (4)$$

The R^2 of the linear fit is 0.65, which suggests a significant correlation between aerosol viscosity and aerosol ERH. This indicates that the influence of organic components on aerosol efflorescence is primarily mediated through their effect on the aerosol viscosity. Interestingly, we found that although aerosol
 185 efflorescence occurs due to the crystallization of inorganic salts, the correlation between aerosol viscosity and the normalized aerosol ERH (ERH/ERH_{Inorg}) was even weaker ($R^2 = 0.59$, Figure S1). Since the



AIOMFAC calculation accounts for inorganic salts, this result emphasizes that the overall aerosol viscosity plays a dominant role in governing efflorescence, overwhelming differences between individual inorganic salts.

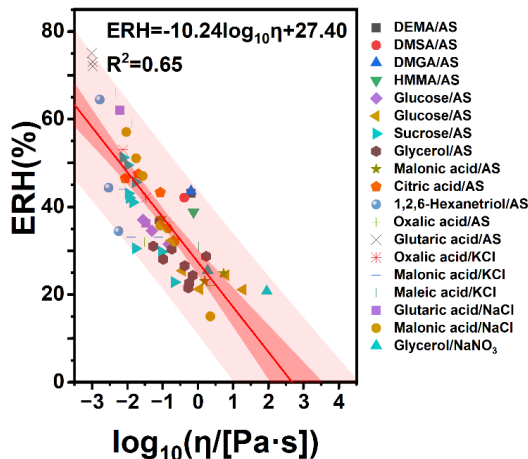
190 Our linear model can predict whether nucleation and crystal growth will occur at a given RH, and whether hygroscopic hysteresis is expected between humidification and dehumidification cycles. Notably, the model predicts that aerosol ERH approaches zero when viscosity reaches 4.76×10^2 Pa·s. We therefore infer that organic-inorganic aerosols with viscosities exceeding 4.76×10^2 Pa·s are unlikely to undergo efflorescence. The complete viscosity-ERH model is expressed as:

$$195 \quad ERH(\eta) = \begin{cases} -10.23 \cdot \log_{10} \eta + 27.4, & \eta < 4.76 \times 10^2 \text{ Pa} \cdot \text{s} \\ 0, & \eta \geq 4.76 \times 10^2 \text{ Pa} \cdot \text{s} \end{cases} \quad (5)$$

We further performed multivariate regression incorporating viscosity ($\log_{10} \eta$), equivalent O:C ratio, ω_{org} , and $T_g(\omega_{\text{org}})$ as independent variables. The four-variable model demonstrated an improved R^2 of 0.69, which is significantly different from the ERH-viscosity model (Sig. F change < 0.05, Table S7) due to the major contribution of viscosity and $T_g(\omega_{\text{org}})$ (both showed $p < 0.05$, Table S7). We therefore 200 established an bivariate viscosity- T_g -ERH model, and the analysis of variance (ANOVA) showed a Sig. F change (0.685) much greater than 0.05 with the same R^2 of 0.69. This indicated that no significant difference between the viscosity- T_g -ERH model and the four-variable model (Table S8), and O:C and ω_{org} did not significantly improve predictive performance. The viscosity- T_g -ERH model is expressed as:

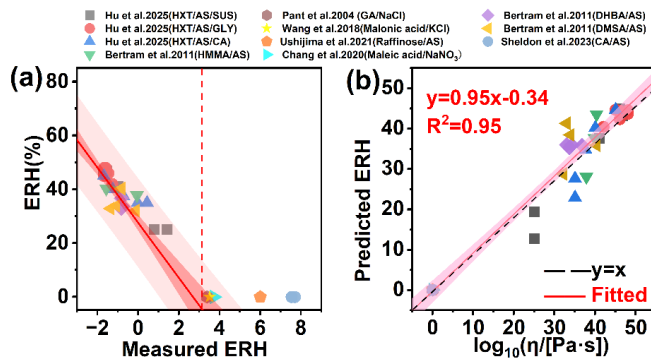
$$RH(\eta, T_g) = 0.25 \cdot T_g(\omega_{\text{org}}) - 12.58 \cdot \log_{10} \eta - 13.28 \quad (6)$$

205 However, the viscosity- T_g -ERH model exhibits practical limitations. The $T_g(\omega_{\text{org}})$ does not account for the possible effects of inorganic salts, as inorganic components do not exhibit a well-defined T_g due to crystallization. Moreover, although adding predictors typically increases coefficient of determination (R^2) by capturing additional variance, the inclusion of T_g improved R^2 by only 0.04. In contrast, the viscosity-ERH model retains strong predictive power, while requiring fewer assumptions, demonstrating broader 210 applicability and greater robustness for predicting ERH across diverse internally mixed organic-inorganic aerosols in the atmosphere.



215 **Figure 2.** Linear fitting of aerosol ERH for different organic-inorganic aerosols by using viscosity ($\log_{10} \eta$) as the predictor. Data points are color- and shape-coded to distinguish between different organic and inorganic aerosol species. The red solid line represents the linear regression fit between viscosity and ERH. The dark pink band indicates the 95% confidence interval, while the light pink band shows the prediction interval. AS refers to ammonium sulfate, DEMA represents Diethyl malonic acid, DMSA represents 2,2-Dimethyl succinic acid, DMGA represents 3,3-Dimethyl glutaric acid, HMMA represents DL-4-Hydroxy-3-methoxymandelic acid and DHBA represents 2,5-Dihydroxybenzoic acid.

220 We then validated the established viscosity-ERH model using an independent validation set (32 data points) compiled from the literature. As depicted in Eq.5, a threshold viscosity of $4.76 \times 10^2 \text{ Pa}\cdot\text{s}$ distinguishes between crystallized and amorphous solid phases in atmospheric aerosols. Figure 3a shows compares the experimentally measured ERH in the validation set with model predictions. For viscosities $< 4.76 \times 10^2 \text{ Pa}\cdot\text{s}$ (data points to the left of the red dashed line), all validation data fall within the predicted 225 confidence intervals, confirming the reliability of using viscosity to predict the ERH of organic-inorganic mixture aerosols. This result suggests that when aerosol viscosity and ambient RH fall below the regression line (red), aerosols tend to undergo nucleation and crystal growth. For viscosities $> 4.76 \times 10^2 \text{ Pa}\cdot\text{s}$ (data points to the right of the red dashed line), consistent with model predictions, aerosols in the validation set remain in a viscous liquid state and ultimately form amorphous solids without 230 crystallization. As shown in Figure 3b, the data points tightly cluster around the $y = x$ reference line (black dashed line), with the fitted line (red solid line) closely aligned and a slope near unity ($R^2 = 0.95$), indicating negligible systematic prediction bias and strong agreement between model predictions and experimental measurements. We also validated the viscosity- T_g -ERH model using the same data set, excluding systems for which T_g could not be estimated. The viscosity- T_g -ERH model also demonstrated 235 good agreement between predicted and measured ERH values (Figure S2)



240 **Figure 3. (a) Comparison between the validation set data and viscosity-ERH model prediction (Eq. 4). (b)**
Comparison of measured ERH values versus model predicted ERH values based on the viscosity-ERH model.
 The black dashed line denotes the $y=x$ reference line, and the red line representing the linear regression fit to
 240 the data, along with the corresponding coefficient of determination (R^2), $R^2=0.95$. The pale pink shading
 represents the 95% confidence interval. DEMA represents Diethyl malonic acid, DMSA represents 2,2-
 Dimethyl succinic acid, DMGA represents 3,3-Dimethyl glutaric acid, HMMA represents DL-4-Hydroxy-3-
 methoxymandelic acid and DHBA represents 2,5-Dihydroxybenzoic acid.

3.3 Nucleation kinetics mechanism for viscosity-dependent ERH

245 Aerosol efflorescence is a kinetically controlled process involving: (1) formation of critical crystal nuclei
 in supersaturated droplets; (2) subsequent crystal growth, and (3) water evaporation(Zhang et al., 2012).
 As demonstrated by Turnbull et al(Turnbull, 1969), viscosity plays a central role in governing nucleation
 rates. In highly viscous aerosols, mass transfer limitations significantly alter nucleation dynamics,
 making nucleus formation the rate-limiting step(Ji et al., 2017b; Wang et al., 2017b). Turnbull et al.
 250 showed that the nucleation rate can be expressed as the product of a pre-exponential factor and two
 thermally activated rate terms(Turnbull, 1969):

$$\tau_x^{-1} = v \exp \left[\frac{-W(T)}{kT} \right] \exp \left[\frac{-\Delta G(T)}{kT} \right] \quad (7)$$

255 where $W(T)$ represents the kinetic barrier associated with atomic rearrangement, and $\Delta G(T)$ is the
 thermodynamic free energy barrier for nucleus formation. The term $\exp(-W(T)/kT)$ represents the
 thermally activated atomic rearrangement rate (i.e., atomic mobility) in liquids and is inversely related
 to viscosity (η^{-1}). Consequently, $\frac{-W(T)}{kT}$ correlates with $-\log \eta$, providing a quantitative link between viscosity and nucleation kinetics. Taking the natural logarithm yields:

$$\ln(\tau_x^{-1}) = -A \log \eta + \ln v - \frac{\Delta G(T)}{kT} \quad (8)$$



where A is a constant linking $-W(T)/kT$ with $-\log\eta$.

260 The empirical relationship between ERH and aerosol viscosity (Eq.4) is consistent with Eq. 8, indicating that $\log_{10}\eta$ serves as a proxy for the kinetic energy barrier $W(T)$, while ERH reflects the effective nucleation rate. The intercept achieved in Eq.4 can therefore be associated with $\ln v - \frac{\Delta G(T)}{kT}$. Overall, the viscosity-ERH model parameterization aligns with this framework, showing that aerosol ERH decreases with increasing $\log\eta$, corresponding to reduced atomic rearrangement rates. Since ambient RH governs 265 aerosol water activity (a_w), the strong correlation between ERH and aerosol viscosity indicates that water activity and molecular mobility jointly control inorganic salt crystallization. Under low water activity, elevated viscosity suppresses molecular rearrangement, hinders nucleus formation, reduces nucleation rates, and consequently suppress or inhibits efflorescence.

4 Conclusions and Implications

270 Our results demonstrate that viscosity is a critical parameter governing aerosol phase-transition kinetics. Although the model incorporating both viscosity and T_g improves explanatory power, the viscosity-ERH model developed herein offers broader applicability for complex atmospheric aerosols, providing a more practical framework for predicting aerosol phase behavior. According to the viscosity-ERH model, efflorescence is completely suppressed when viscosity exceeds $4.76 \times 10^2 \text{ Pa}\cdot\text{s}$.

275 Regional viscosity predictions by Zhang et al suggest that in southern and northeastern China,(Zhang et al., 2024) SOA are predominantly liquid or have low viscosities ($<10^4 \text{ Pa s}$); in central and northeastern China, SOA typically exhibit semi-solid viscosities ($10^5 - 10^8 \text{ Pa s}$); while highly viscous or glassy SOA ($\eta > 10^8 \text{ Pa s}$) are mainly present in the northwest.

280 Although SOA viscosity may significantly increase by several orders of magnitude as water activity (and consequently aerosol water content) decreases, (Hosny et al., 2016b; Renbaum-Wolff et al., 2013; Saukko et al., 2012; Song et al., 2016a; Yli-Juuti et al., 2017) SOA tend to become more oxidized and internally mixed with secondary inorganic aerosols during atmospheric aging. This aging process significantly lowers the overall viscosity of SOA due to the greater hygroscopicity of more oxygenated organics and inorganic salts.(Dette and Koop, 2015) Consequently, in more developed and urbanized regions like 285 southern and northeastern China, atmospheric aerosols are more likely to undergo efflorescence and crystallization, leading to hysteresis in aerosol size and water contents during humidification and dehumidification processes. The hysteresis induced by aerosol efflorescence has important implications



for modeling aerosol size evolution, optical properties, and chemical reactivity.

It is important to note that the aerosol viscosities in this study were derived from thermodynamic model
290 predictions, as in-situ measurement techniques for atmospheric aerosol viscosity remain largely
unavailable. Although substrate-based methods—such as poke-flow cytometry and fluorescence lifetime
imaging microscopy (FLIM)—have been successfully employed to determine SOA viscosity under
laboratory conditions, substrate effects must be carefully considered.(Grayson et al., 2015; Hosny et al.,
2013) This highlights an urgent need to develop techniques that can directly measure aerosol viscosity at
295 a given RH in ambient environments and to validate viscosity-dependent phase transition predictions.

Optical tweezer is a promising tool for quantitative viscosity measurements of levitated particles;
however, the technique requires further advancement to measure submicron organic aerosols in real
atmospheric conditions(Jonathan P. Reid et al., 2014). In conclusion, improving predictive tools for
aerosol phase state and advancing viscosity parameterizations in global climate models will be essential
300 to enhance our understanding of the impacts of aerosol phase state on climate and air quality.

Code and data availability

The data supporting this article have been included in the main text and as part of the Supplementary
Information: Tables S1-S8, Fig. S1-S2.

Supplement

305 The supplement related to this article is available online at:

Author contributions

SC and QH analyzed and visualized the data and wrote the original draft. SC conducted the
experiments and model calculations. QH created the original research framework. QH and YL
reviewed and edited the paper. QH, PL, and YZ supervised the study. All authors discussed the
310 results and contributed to the article editing.

Competing interests

The contact author has declared that neither they nor their co-author has any competing interests.



Acknowledgements

We gratefully acknowledge the foundational model developed by Dr. Andreas Zuend, which served as
315 an essential tool for our viscosity calculations. We also thank Dr. Ying Li for providing feedback on an
earlier draft of the manuscript. During the preparation of this work the authors used Generative Pretrained
Transformer 4 (GPT-4) to detect and correct grammatical errors in the draft. After using this tool/service,
the authors reviewed and edited the content as needed and take full responsibility for the content of the
publication.

320 Financial support

This study was supported by the National Natural Science Foundation of China (No. 22406010,
42127806, and 42075110)

References

Armeli, G., Peters, J.-H., and Koop, T.: Machine-Learning-Based Prediction of the Glass Transition
325 Temperature of Organic Compounds Using Experimental Data, *ACS Omega*, 8, 12298–12309,
<https://doi.org/10.1021/acsomega.2c08146>, 2023.

Berkemeier, T., Steimer, S. S., Krieger, U. K., Peter, T., Pöschl, U., Ammann, M., and Shiraiwa, M.:
Ozone uptake on glassy, semi-solid and liquid organic matter and the role of reactive oxygen
intermediates in atmospheric aerosol chemistry, *Phys. Chem. Chem. Phys.*, 18, 12662–12674,
330 <https://doi.org/10.1039/C6CP00634E>, 2016.

Bertram, A. K., Martin, S. T., Hanna, S. J., Smith, M. L., Bodsworth, A., Chen, Q., Kuwata, M., Liu, A.,
You, Y., and Zorn, S. R.: Predicting the relative humidities of liquid-liquid phase separation, efflorescence,
and deliquescence of mixed particles of ammonium sulfate, organic material, and water using the
organic-to-sulfate mass ratio of the particle and the oxygen-to-carbon elemental ratio of the organic
335 component, *Atmospheric Chemistry and Physics*, 11, 10995–11006, <https://doi.org/10.5194/acp-11-10995-2011>, 2011.

Boreddy, S. K. R., Kawamura, K., Mkoma, S., and Fu, P.: Hygroscopic behavior of water-soluble matter



extracted from biomass burning aerosols collected at a rural site in Tanzania, East Africa, *Journal of Geophysical Research: Atmospheres*, 119, 12,233–12,245, <https://doi.org/10.1002/2014JD021546>, 2014.

340 Braban, C. F. and Abbatt, J. P. D.: A study of the phase transition behavior of internally mixed ammonium sulfate-malonic acid aerosols, *Atmospheric Chemistry and Physics*, 4, 1451–1459, <https://doi.org/10.5194/acp-4-1451-2004>, 2004.

Cai, C., Luan, Y., Shi, X., and Zhang, Y.: $(\text{NH}_4)_2\text{SO}_4$ heterogeneous nucleation and glycerol evaporation of $(\text{NH}_4)_2\text{SO}_4$ -glycerol system in its dynamic efflorescence process, *Chemical Physics*, 483–484, 140–148, <https://doi.org/10.1016/j.chemphys.2016.12.003>, 2017.

345 Chang, P.: Study on single aerosol particle by spontaneous and stimulated Raman spectroscopy. Ph.D. Dissertation, Beijing Institute of Technology., 2020.

Choi, M. Y. and Chan, C. K.: The effects of organic species on the hygroscopic behaviors of inorganic aerosols, *Environ. Sci. Technol.*, 36, 2422–2428, <https://doi.org/10.1021/es0113293>, 2002.

350 Davis, R. D., Lance, S., Gordon, J. A., Ushijima, S. B., and Tolbert, M. A.: Contact efflorescence as a pathway for crystallization of atmospherically relevant particles, *Proc Natl Acad Sci U S A*, 112, 15815–15820, <https://doi.org/10.1073/pnas.1522860113>, 2015.

DeRieux, W.-S. W., Li, Y., Lin, P., Laskin, J., Laskin, A., Bertram, A. K., Nizkorodov, S. A., and Shiraiwa, M.: Predicting the glass transition temperature and viscosity of secondary organic material using 355 molecular composition, *Atmospheric Chemistry and Physics*, 18, 6331–6351, <https://doi.org/10.5194/acp-18-6331-2018>, 2018.

Dette, H. P. and Koop, T.: Glass Formation Processes in Mixed Inorganic/Organic Aerosol Particles, *J. Phys. Chem. A*, 119, 4552–4561, <https://doi.org/10.1021/jp5106967>, 2015.

360 Donahue, N. M., Epstein, S. A., Pandis, S. N., and Robinson, A. L.: A two-dimensional volatility basis set: 1. organic-aerosol mixing thermodynamics, *Atmospheric Chemistry and Physics*, 11, 3303–3318, <https://doi.org/10.5194/acp-11-3303-2011>, 2011.

Fan, J., Comstock, J. M., and Ovchinnikov, M.: The cloud condensation nuclei and ice nuclei effects on tropical anvil characteristics and water vapor of the tropical tropopause layer, *Environ. Res. Lett.*, 5, 044005, <https://doi.org/10.1088/1748-9326/5/4/044005>, 2010.

365 Fard, M. M., Krieger, U. K., and Peter, T.: Shortwave radiative impact of liquid–liquid phase separation in brown carbon aerosols, *Atmospheric Chemistry and Physics*, 18, 13511–13530, <https://doi.org/10.5194/acp-18-13511-2018>, 2018.



Fitzgerald, C., Hosny, N. A., Tong, H., Seville, P. C., Gallimore, P. J., Davidson, N. M., Athanasiadis, A., Botchway, S. W., Ward, A. D., Kalberer, M., Kuimova, M. K., and Pope, F. D.: Fluorescence lifetime imaging of optically levitated aerosol: a technique to quantitatively map the viscosity of suspended aerosol particles, *Phys Chem Chem Phys*, 18, 21710–21719, <https://doi.org/10.1039/c6cp03674k>, 2016.

370 Fredenslund, A., Jones, R. L., and Prausnitz, J. M.: Group-contribution estimation of activity coefficients in nonideal liquid mixtures, *AIChE Journal*, 21, 1086–1099, <https://doi.org/10.1002/aic.690210607>, 1975.

375 Freedman, M. A., Huang, Q., and Pitta, K. R.: Phase Transitions in Organic and Organic/Inorganic Aerosol Particles, *Annual Review of Physical Chemistry*, 75, 257–281, <https://doi.org/10.1146/annurev-physchem-083122-115909>, 2024.

Galeazzo, T. and Shiraiwa, M.: Predicting glass transition temperature and melting point of organic compounds via machine learning and molecular embeddings, <https://doi.org/10.1039/D1EA00090J>, 380 2022.

Ghorai, S., Wang, B., Tivanski, A., and Laskin, A.: Hygroscopic properties of internally mixed particles composed of NaCl and water-soluble organic acids, *Environ. Sci. Technol.*, 48, 2234–2241, <https://doi.org/10.1021/es404727u>, 2014.

Gordon, M. and Taylor, J. S.: Ideal copolymers and the second-order transitions of synthetic rubbers. i. 385 non-crystalline copolymers, *Journal of Applied Chemistry*, 2, 493–500, <https://doi.org/10.1002/jctb.5010020901>, 1952.

Grayson, J. W., Song, M., Sellier, M., and Bertram, A. K.: Validation of the poke-flow technique combined with simulations of fluid flow for determining viscosities in samples with small volumes and high viscosities, *Atmospheric Measurement Techniques*, 8, 2463–2472, <https://doi.org/10.5194/amt-8-2463-2015>, 2015.

390 Guo, Y., Wang, N., Pang, S., and Zhang, Y.: Hygroscopic properties and compositional evolution of internally mixed sodium nitrate-amino acid aerosols, *Atmospheric Environment*, 242, 117848, <https://doi.org/10.1016/j.atmosenv.2020.117848>, 2020.

Hallquist, M., Wenger, J. C., Baltensperger, U., Rudich, Y., Simpson, D., Claeys, M., Dommen, J., 395 Donahue, N. M., George, C., Goldstein, A. H., Hamilton, J. F., Herrmann, H., Hoffmann, T., Iinuma, Y., Jang, M., Jenkin, M. E., Jimenez, J. L., Kiendler-Scharr, A., Maenhaut, W., McFiggans, G., Mentel, T. F., Monod, A., Prévôt, A. S. H., Seinfeld, J. H., Surratt, J. D., Szmigielski, R., and Wildt, J.: The formation,



properties and impact of secondary organic aerosol: current and emerging issues, *Atmospheric Chemistry and Physics*, 9, 5155–5236, <https://doi.org/10.5194/acp-9-5155-2009>, 2009.

400 Hansen, H. K., Rasmussen, P., Fredenslund, A., Schiller, M., and Gmehling, J.: Vapor-liquid equilibria by UNIFAC group contribution. 5. Revision and extension, *Ind. Eng. Chem. Res.*, 30, 2352–2355, <https://doi.org/10.1021/ie00058a017>, 1991.

Hosny, N. A., Fitzgerald, C., Tong, C., Kalberer, M., Kuimova, M. K., and Pope, F. D.: Fluorescent lifetime imaging of atmospheric aerosols: a direct probe of aerosol viscosity, *Faraday Discuss.*, 165, 343–356, <https://doi.org/10.1039/C3FD00041A>, 2013.

405 Hosny, N. A., Fitzgerald, C., Vyšniauskas, A., Athanasiadis, A., Berkemeier, T., Uygur, N., Pöschl, U., Shiraiwa, M., Kalberer, M., Pope, F. D., and Kuimova, M. K.: Direct imaging of changes in aerosol particle viscosity upon hydration and chemical aging, *Chem. Sci.*, 7, 1357–1367, <https://doi.org/10.1039/c5sc02959g>, 2016a.

410 Hosny, N. A., Fitzgerald, C., Vyšniauskas, A., Athanasiadis, A., Berkemeier, T., Uygur, N., Pöschl, U., Shiraiwa, M., Kalberer, M., Pope, F. D., and Kuimova, M. K.: Direct imaging of changes in aerosol particle viscosity upon hydration and chemical aging, *Chem. Sci.*, 7, 1357–1367, <https://doi.org/10.1039/C5SC02959G>, 2016b.

Hu, S., Fan, R., Wu, L., Li, Y., Zhang, B., Yuan, Z., Li, Q., Ma, S., Zhao, Z., and Xu, T.: Influence of 415 Amorphous Humic Acid Solids on the Phase Transition Behavior of Nitrate Aerosols, *J. Phys. Chem. A*, <https://doi.org/10.1021/acs.jpca.5c03039>, 2025.

Huang, Q., Pitta, K. R., Constantini, K., Ott, E.-J. E., Zuend, A., and Freedman, M. A.: Experimental phase diagram and its temporal evolution for submicron 2-methylglutaric acid and ammonium sulfate aerosol particles, *Phys. Chem. Chem. Phys.*, 26, 2887–2894, <https://doi.org/10.1039/D3CP04411D>, 2024.

420 Ji, Z.-R., Zhang, Y., Pang, S.-F., and Zhang, Y.-H.: Crystal Nucleation and Crystal Growth and Mass Transfer in Internally Mixed Sucrose/NaNO₃ Particles, *J. Phys. Chem. A*, 121, 7968–7975, <https://doi.org/10.1021/acs.jpca.7b08004>, 2017a.

Ji, Z.-R., Zhang, Y., Pang, S.-F., and Zhang, Y.-H.: Crystal Nucleation and Crystal Growth and Mass Transfer in Internally Mixed Sucrose/NaNO₃ Particles, *J. Phys. Chem. A*, 121, 7968–7975, 425 <https://doi.org/10.1021/acs.jpca.7b08004>, 2017b.

Jonathan P. Reid, Rory M. Power, Chen Cai, and Stephen H. Simpson: Micro-rheology and interparticle interactions in aerosols probed with optical tweezers, *Proc. SPIE*, 91641W,



<https://doi.org/10.1117/12.2061018>, 2014.

Knopf, D. A. and Alpert, P. A.: Atmospheric ice nucleation, *Nat Rev Phys*, 5, 203–217,

430 <https://doi.org/10.1038/s42254-023-00570-7>, 2023.

Kohl, I., Bachmann, L., Hallbrucker, A., Mayer, E., and Loerting, T.: Liquid-like relaxation in hyperquenched water at ≤ 140 K, *Phys. Chem. Chem. Phys.*, 7, 3210–3220, <https://doi.org/10.1039/B507651J>, 2005.

Koop, T., Bookhold, J., Shiraiwa, M., and Pöschl, U.: Glass transition and phase state of organic

435 compounds: dependency on molecular properties and implications for secondary organic aerosols in the atmosphere, *Phys. Chem. Chem. Phys.*, 13, 19238–19255, <https://doi.org/10.1039/C1CP22617G>, 2011a.

Koop, T., Bookhold, J., Shiraiwa, M., and Pöschl, U.: Glass transition and phase state of organic compounds: dependency on molecular properties and implications for secondary organic aerosols in the atmosphere, *Phys. Chem. Chem. Phys.*, 13, 19238–19255, <https://doi.org/10.1039/C1CP22617G>, 2011b.

440 Laskina, O., Morris, H. S., Grandquist, J. R., Qin, Z., Stone, E. A., Tivanski, A. V., and Grassian, V. H.: Size matters in the water uptake and hygroscopic growth of atmospherically relevant multicomponent aerosol particles, *J. Phys. Chem. A*, 119, 4489–4497, <https://doi.org/10.1021/jp510268p>, 2015.

Li, Y., Pöschl, U., and Shiraiwa, M.: Molecular corridors and parameterizations of volatility in the chemical evolution of organic aerosols, *Atmospheric Chemistry and Physics*, 16, 3327–3344,

445 <https://doi.org/10.5194/acp-16-3327-2016>, 2016.

Li, Y., Day, D. A., Stark, H., Jimenez, J. L., and Shiraiwa, M.: Predictions of the glass transition temperature and viscosity of organic aerosols from volatility distributions, *Atmospheric Chemistry and Physics*, 20, 8103–8122, <https://doi.org/10.5194/acp-20-8103-2020>, 2020a.

Li, Y., Day, D. A., Stark, H., Jimenez, J. L., and Shiraiwa, M.: Predictions of the glass transition

450 temperature and viscosity of organic aerosols from volatility distributions, *Atmospheric Chemistry and Physics*, 20, 8103–8122, <https://doi.org/10.5194/acp-20-8103-2020>, 2020b.

Lilek, J. and Zuend, A.: A predictive viscosity model for aqueous electrolytes and mixed organic–inorganic aerosol phases, *Atmospheric Chemistry and Physics*, 22, 3203–3233, <https://doi.org/10.5194/acp-22-3203-2022>, 2022a.

455 Lilek, J. and Zuend, A.: A predictive viscosity model for aqueous electrolytes and mixed organic–inorganic aerosol phases, *Atmospheric Chemistry and Physics*, 22, 3203–3233, <https://doi.org/10.5194/acp-22-3203-2022>, 2022b.



Ma, S., Pang, S., Li, J., and Zhang, Y.: A review of efflorescence kinetics studies on atmospherically relevant particles, *Chemosphere*, 277, 130320, <https://doi.org/10.1016/j.chemosphere.2021.130320>, 2021a.

Ma, S., Chen, Z., Pang, S., and Zhang, Y.: Observations on hygroscopic growth and phase transitions of mixed 1, 2, 6-hexanetriol/ $(\text{NH}_4)_2\text{SO}_4$ particles: investigation of the liquid–liquid phase separation (LLPS) dynamic process and mechanism and secondary LLPS during the dehumidification, *Atmospheric Chemistry and Physics*, 21, 9705–9717, <https://doi.org/10.5194/acp-21-9705-2021>, 2021b.

Mikhailov, E., Vlasenko, S., Martin, S. T., Koop, T., and Pöschl, U.: Amorphous and crystalline aerosol particles interacting with water vapor: conceptual framework and experimental evidence for restructuring, phase transitions and kinetic limitations, *Atmospheric Chemistry and Physics*, 9, 9491–9522, <https://doi.org/10.5194/acp-9-9491-2009>, 2009.

Novo, N., Carotenuto, A., Mensitieri, G., Fraldi, M., and Pugno, N.: Modeling of virus survival time in respiratory droplets on surfaces: a new rational approach for antivirus strategies, *Frontiers in Materials*, 8, 631723, <https://doi.org/10.3389/fmats.2021.631723>, 2021.

Oswin, H. P., Haddrell, A. E., Otero-Fernandez, M., Mann, J. F. S., Cogan, T. A., Hilditch, T. G., Tian, J., Hardy, D., Hill, D. J., Finn, A., Davidson, A. D., and Reid, J. P.: Reply to Klein et al.: The importance of aerosol pH for airborne respiratory virus transmission, *Proc Natl Acad Sci U S A*, 119, e2212556119, <https://doi.org/10.1073/pnas.2212556119>, 2022.

Pant, A., Fok, A., Parsons, M. T., Mak, J., and Bertram, A. K.: Deliquescence and crystallization of ammonium sulfate-glutaric acid and sodium chloride-glutaric acid particles, *Geophysical Research Letters*, 31, 2004GL020025, <https://doi.org/10.1029/2004GL020025>, 2004.

Parsons, M. T., Knopf, D. A., and Bertram, A. K.: Deliquescence and crystallization of ammonium sulfate particles internally mixed with water-soluble organic compounds, *J. Phys. Chem. A*, 108, 11600–11608, <https://doi.org/10.1021/jp0462862>, 2004.

Pöschl, U.: Atmospheric aerosols: composition, transformation, climate and health effects, *Angewandte Chemie International Edition*, 44, 7520–7540, <https://doi.org/10.1002/anie.200501122>, 2005.

Reid, J. P., Bertram, A. K., Topping, D. O., Laskin, A., Martin, S. T., Petters, M. D., Pope, F. D., and Rovelli, G.: The viscosity of atmospherically relevant organic particles, *Nat Commun*, 9, 956, <https://doi.org/10.1038/s41467-018-03027-z>, 2018.

Ren, H.-M., Cai, C., Leng, C.-B., Pang, S.-F., and Zhang, Y.-H.: Nucleation Kinetics in Mixed



NaNO₃/Glycerol Droplets Investigated with the FTIR–ATR Technique, *J. Phys. Chem. B*, 120, 2913–2920, <https://doi.org/10.1021/acs.jpcb.5b12442>, 2016.

490 Renbaum-Wolff, L., Grayson, J. W., Bateman, A. P., Kuwata, M., Sellier, M., Murray, B. J., Shilling, J. E., Martin, S. T., and Bertram, A. K.: Viscosity of α -pinene secondary organic material and implications for particle growth and reactivity, *Proceedings of the National Academy of Sciences*, 110, 8014–8019, <https://doi.org/10.1073/pnas.1219548110>, 2013.

Saukko, E., Lambe, A. T., Massoli, P., Koop, T., Wright, J. P., Croasdale, D. R., Pedernera, D. A., Onasch, T. B., Laaksonen, A., Davidovits, P., Worsnop, D. R., and Virtanen, A.: Humidity-dependent phase state of SOA particles from biogenic and anthropogenic precursors, *Atmospheric Chemistry and Physics*, 12, 7517–7529, <https://doi.org/10.5194/acp-12-7517-2012>, 2012.

495 Shi, X.-M., Wu, F.-M., Jing, B., Wang, N., Xu, L.-L., Pang, S.-F., and Zhang, Y.-H.: Hygroscopicity of internally mixed particles composed of (NH₄)₂SO₄ and citric acid under pulsed RH change, *Chemosphere*, 188, 532–540, <https://doi.org/10.1016/j.chemosphere.2017.09.024>, 2017.

Shiraiwa, M., Zuend, A., Bertram, A. K., and Seinfeld, J. H.: Gas-article partitioning of atmospheric aerosols: interplay of physical state, non-ideal mixing and morphology, *Phys. Chem. Chem. Phys.*, 15, 11441–11453, <https://doi.org/10.1039/C3CP51595H>, 2013.

500 Shiraiwa, M., Li, Y., Tsimpidi, A. P., Karydis, V. A., Berkemeier, T., Pandis, S. N., Lelieveld, J., Koop, T., and Pöschl, U.: Global distribution of particle phase state in atmospheric secondary organic aerosols, *Nat Commun*, 8, 15002, <https://doi.org/10.1038/ncomms15002>, 2017.

Shrivastava, M., Cappa, C. D., Fan, J., Goldstein, A. H., Guenther, A. B., Jimenez, J. L., Kuang, C., Laskin, A., Martin, S. T., Ng, N. L., Petaja, T., Pierce, J. R., Rasch, P. J., Roldin, P., Seinfeld, J. H., Shilling, J., Smith, J. N., Thornton, J. A., Volkamer, R., Wang, J., Worsnop, D. R., Zaveri, R. A., Zelenyuk, A., and Zhang, Q.: Recent advances in understanding secondary organic aerosol: Implications for global climate forcing, *Reviews of Geophysics*, 55, 509–559, <https://doi.org/10.1002/2016RG000540>, 2017.

510 Smith, J. N., Draper, D. C., Chee, S., Dam, M., Glicker, H., Myers, D., Thomas, A. E., Lawler, M. J., and Myllys, N.: Atmospheric clusters to nanoparticles: Recent progress and challenges in closing the gap in chemical composition, *Journal of Aerosol Science*, 153, 105733, <https://doi.org/10.1016/j.jaerosci.2020.105733>, 2021.

Song, M., Liu, P. F., Hanna, S. J., Zaveri, R. A., Potter, K., You, Y., Martin, S. T., and Bertram, A. K.: Relative humidity-dependent viscosity of secondary organic material from toluene photo-oxidation and



possible implications for organic particulate matter over megacities, *Atmospheric Chemistry and Physics*, 16, 8817–8830, <https://doi.org/10.5194/acp-16-8817-2016>, 2016a.

520 Song, Y. C., Haddrell, A. E., Bzdek, B. R., Reid, J. P., Bannan, T., Topping, D. O., Percival, C., and Cai, C.: Measurements and Predictions of Binary Component Aerosol Particle Viscosity, *J. Phys. Chem. A*, 120, 8123–8137, <https://doi.org/10.1021/acs.jpca.6b07835>, 2016b.

S. Sheldon, C., M. Choczynski, J., Morton, K., Diaz, T. P., D. Davis, R., and F. Davies, J.: Exploring the hygroscopicity, water diffusivity, and viscosity of organic–inorganic aerosols – a case study on internally-mixed citric acid and ammonium sulfate particles, *Environmental Science: Atmospheres*, 3, 24–34, <https://doi.org/10.1039/D2EA00116K>, 2023.

Tong, H.-J., Reid, J. P., Bones, D. L., Luo, B. P., and Krieger, U. K.: *Atmospheric Chemistry and Physics*, 11, 4739–4754, <https://doi.org/10.5194/acp-11-4739-2011>, 2011.

Turnbull, D.: Under what conditions can a glass be formed?, *Contemporary Physics*, 530 <https://doi.org/10.1080/00107516908204405>, 1969.

Ushijima, S. B., Huynh, E., Davis, R. D., and Tolbert, M. A.: Seeded crystal growth of internally mixed organic–inorganic aerosols: impact of organic phase state, *J. Phys. Chem. A*, 125, 8668–8679, <https://doi.org/10.1021/acs.jpca.1c04471>, 2021.

535 Virtanen, A., Joutsensaari, J., Koop, T., Kannisto, J., Yli-Pirilä, P., Leskinen, J., Mäkelä, J. M., Holopainen, J. K., Pöschl, U., Kulmala, M., Worsnop, D. R., and Laaksonen, A.: An amorphous solid state of biogenic secondary organic aerosol particles, *Nature*, 467, 824–827, <https://doi.org/10.1038/nature09455>, 2010.

Wang, L.-N., Cai, C., and Zhang, Y.-H.: Correction to “Kinetically Determined Hygroscopicity and Efflorescence of Sucrose–Ammonium Sulfate Aerosol Droplets under Lower Relative Humidity,” *J. Phys.*

540 *Chem. B*, 121, 11018–11018, <https://doi.org/10.1021/acs.jpcb.7b10848>, 2017a.

Wang, L.-N., Cai, C., and Zhang, Y.-H.: Kinetically Determined Hygroscopicity and Efflorescence of Sucrose–Ammonium Sulfate Aerosol Droplets under Lower Relative Humidity, *J. Phys. Chem. B*, 121, 8551–8557, <https://doi.org/10.1021/acs.jpcb.7b05551>, 2017b.

545 Wang, X.: Study on the hygroscopicity of mixed aerosols composed of organic acids and inorganic salts by Raman spectroscopy. Ph.D. Dissertation, Beijing Institute of Technology., 2018.

Wang, X., Jing, B., Tan, F., Ma, J., Zhang, Y., and Ge, M.: Hygroscopic behavior and chemical composition evolution of internally mixed aerosols composed of oxalic acid and ammonium sulfate,



Atmospheric Chemistry and Physics, 17, 12797–12812, <https://doi.org/10.5194/acp-17-12797-2017>,
2017c.

550 Wu, F.: Thermodynamics and Kinetics Research of Mixed Inorganic/Glutaric acid Aerosols in the
Hygroscopic Process. Ph.D. Dissertation, Beijing Institute of Technology., 2017.

Xu, Y., Liu, P., Ma, S., Pei, W., Pang, S., and Zhang, Y.: Efflorescence kinetics of aerosols comprising
internally-mixed ammonium sulfate and water-soluble organic compounds, Atmospheric Environment,
274, 119007, <https://doi.org/10.1016/j.atmosenv.2022.119007>, 2022.

555 Yli-Juuti, T., Pajunoja, A., Tikkainen, O.-P., Buchholz, A., Faiola, C., Väistönen, O., Hao, L., Kari, E.,
Peräkylä, O., Garmash, O., Shiraiwa, M., Ehn, M., Lehtinen, K., and Virtanen, A.: Factors controlling
the evaporation of secondary organic aerosol from α -pinene ozonolysis, Geophysical Research Letters,
44, 2562–2570, <https://doi.org/10.1002/2016GL072364>, 2017.

Yu, J.-Y., Zhang, Y., Zeng, G., Zheng, C.-M., Liu, Y., and Zhang, Y.-H.: Suppression of NaNO₃ Crystal
560 Nucleation by Glycerol: Micro-Raman Observation on the Efflorescence Process of Mixed
Glycerol/NaNO₃/Water Droplets, J. Phys. Chem. B, 116, 1642–1650, <https://doi.org/10.1021/jp210824e>,
2012.

Yu, Z., Jang, M., and Madhu, A.: Prediction of phase state of secondary organic aerosol internally mixed
with aqueous inorganic salts, J. Phys. Chem. A, 125, 10198–10206,
565 <https://doi.org/10.1021/acs.jpca.1c06773>, 2021.

Zhang, R., Khalizov, A., Wang, L., Hu, M., and Xu, W.: Nucleation and growth of nanoparticles in the
atmosphere, Chem. Rev., 112, 1957–2011, <https://doi.org/10.1021/cr2001756>, 2012.

Zhang, Y., Nichman, L., Spencer, P., Jung, J. I., Lee, A., Heffernan, B. K., Gold, A., Zhang, Z., Chen, Y.,
Canagaratna, M. R., Jayne, J. T., Worsnop, D. R., Onasch, T. B., Surratt, J. D., Chandler, D., Davidovits,
570 P., and Kolb, C. E.: The Cooling Rate- and Volatility-Dependent Glass-Forming Properties of Organic
Aerosols Measured by Broadband Dielectric Spectroscopy, Environ. Sci. Technol., 53, 12366–12378,
<https://doi.org/10.1021/acs.est.9b03317>, 2019.

Zhang, Z., Li, Y., Ran, H., An, J., Qu, Y., Zhou, W., Xu, W., Hu, W., Xie, H., Wang, Z., Sun, Y., and
Shiraiwa, M.: Simulated phase state and viscosity of secondary organic aerosols over China, Atmospheric
575 Chemistry and Physics, 24, 4809–4826, <https://doi.org/10.5194/acp-24-4809-2024>, 2024.

Zobrist, B., Marcolli, C., Pedernera, D. A., and Koop, T.: Do atmospheric aerosols form glasses?,
Atmospheric Chemistry and Physics, 8, 5221–5244, <https://doi.org/10.5194/acp-8-5221-2008>, 2008.



Zobrist, B., Soonsin, V., Luo, B. P., Krieger, U. K., Marcolli, C., Peter, T., and Koop, T.: Ultra-slow water diffusion in aqueous sucrose glasses, *Phys. Chem. Chem. Phys.*, 13, 3514–3526,
580 <https://doi.org/10.1039/C0CP01273D>, 2011.

Zuend, A., Marcolli, C., Luo, B. P., and Peter, T.: A thermodynamic model of mixed organic-inorganic aerosols to predict activity coefficients, *Atmospheric Chemistry and Physics*, 8, 4559–4593,
<https://doi.org/10.5194/acp-8-4559-2008>, 2008.

Zuend, A., Marcolli, C., Booth, A. M., Lienhard, D. M., Soonsin, V., Krieger, U. K., Topping, D. O.,
585 McFiggans, G., Peter, T., and Seinfeld, J. H.: New and extended parameterization of the thermodynamic model AIOMFAC: calculation of activity coefficients for organic-inorganic mixtures containing carboxyl, hydroxyl, carbonyl, ether, ester, alkenyl, alkyl, and aromatic functional groups, *Atmospheric Chemistry and Physics*, 11, 9155–9206, <https://doi.org/10.5194/acp-11-9155-2011>, 2011a.

Zuend, A., Marcolli, C., Booth, A. M., Lienhard, D. M., Soonsin, V., Krieger, U. K., Topping, D. O.,
590 McFiggans, G., Peter, T., and Seinfeld, J. H.: New and extended parameterization of the thermodynamic model AIOMFAC: calculation of activity coefficients for organic-inorganic mixtures containing carboxyl, hydroxyl, carbonyl, ether, ester, alkenyl, alkyl, and aromatic functional groups, *Atmospheric Chemistry and Physics*, 11, 9155–9206, <https://doi.org/10.5194/acp-11-9155-2011>, 2011b.

595